

Synthesis and characterization of new triphenylamine-based dyes with novel anchoring groups for dye-sensitized solar cell applications

Alireza Salimi Beni¹ · Behzad Hosseinzadeh¹ · Masoume Azari¹ · Raheleh Ghahary²

Received: 13 May 2016 / Accepted: 24 September 2016 / Published online: 9 November 2016
© Springer Science+Business Media New York 2016

Abstract Three new chromophores based on the triphenylamine (MM, DM, DN) with various novel electron withdrawing anchoring groups have been synthesized for use in dye-sensitized solar cells (DSSCs). The sensitizers were characterized by ¹H and ¹³C NMR, Mass, UV–Vis, and electrochemical analysis. The HOMO and LUMO electron distributions of the sensitizers were calculated using density functional theory on a B3LYP level for geometry optimization. The DSSC device based on DM dye showed the best photovoltaic performance among MM and DN dyes: maximum monochromatic incident photon-to-current conversion efficiency (IPCE) of 98 %, short circuit current (J_{SC}) of 4.58 mA/cm², open circuit voltage (V_{OC}) of 0.62 V, fill factor (FF) of 0.77, and overall power conversion efficiency (PCE) of 2.01 %. The results reveal that the difference in number and type of anchoring groups of the dyes significantly influence the photovoltaic performance of their DSSCs.

1 Introduction

Since the beginning of the 21st century, depletion of fossil fuel reserve and global warming have become important worldwide issues, which motivate researcher for tremendous growth of investigations on environmental friendly

new energy sources as well as more efficient energy conversion and storage.

It is well-known that solar energy is the largest renewable carbon-free resource. Among the devices that can convert solar energy into electricity, dye-sensitized solar cells (DSSCs) have gained widespread interest due to their high-energy conversion efficiency and low production cost [1]. Although the conventional ruthenium-based sensitizers (such as N3/N719) [2, 3] and the black dye [4] hold the record of the solar-energy-to-electricity conversion efficiencies of 11 % under AM 1.5 irradiation, they are expensive and hard to purify relative to metal-free organic sensitizers. On the other hand, DSSCs based on metal-free organic dyes have many advantages in lower cost, easier structural modification, and higher molar extinction coefficient of the dyes, and consequently, they have been considered as an excellent alternative for organometallic complex-based DSSCs. Conversion efficiency surpassing 10 % has been demonstrated for a metal-free sensitizer based DSSC [5]. Still, a more strategic molecular design of organic sensitizers is required to achieve higher efficiency (η) values. The requirements [6–8] of efficient sensitizers for use in DSSCs include (a) wide absorption range and high absorption coefficient that give high light harvesting efficiency, (b) excited-state redox potential should match the energy of the conduction band, (c) light excitation associated with vectorial electron flow from the light-harvesting moiety of the sensitizer towards the surface of the semiconductor, (d) conjugation across the donor and the anchoring group, (e) good anchoring group and, (f) electronic coupling between the lowest unoccupied molecular orbital (LUMO) of the sensitizer and the TiO₂ conduction band. The major factors that result in low conversion efficiency of many organic sensitizers in the DSSCs are (a) the aggregation of sensitizer on the semiconductor surface and (b) recombination of conduction-band electrons with the iodide/triiodide redox

✉ Alireza Salimi Beni
salimibeni@yu.ac.ir

Behzad Hosseinzadeh
behzad.hosseinzadeh89@gmail.com

¹ Chemistry Department, Yasouj University,
Yasouj 75918-74831, Iran

² Department of Physics, Sharif University of Technology,
Tehran, Iran

mediator [9]. The organic dyes commonly consist of conjugated systems comprising donor, linker, and acceptor groups (i.e., a D- π -A molecular structure). Their various properties could be finely tuned by altering independently or matching the different groups of D- π -A dyes. Triphenylamine, fluorene, thiophene, indoline, merocyanine, coumarin, etc. have been employed as donor units in the development of metal-free sensitizers and exhibit promising device characteristics [10–13]. The excellent stability, electron-donating ability and aggregation resistance due to a non-planar molecular configuration of especially triphenylamine (TPA)-based sensitizers have made them prospective candidates for DSSC applications. The reduced aggregation of TPA-based sensitizers facilitates the ultrafast interfacial electron injection from excited dye molecules to the conduction band of the semiconductor. Secondly, the recombination of injected electrons with the redox couple can be suppressed, due to the propeller-shaped TPA molecular structure. In addition, the oxidized TPA unit is spatially conveniently placed for the approach of the redox couple species, ensuring fast dye regeneration.

In this article we designed three (D- π -A) sensitizers with triphenylamine as the donor, Meldrum's acid and 4-nitrophenylacetic acid as acceptor/anchor. All the new triphenylamine dyes were synthesized and characterized by spectroscopic techniques. The impact of different anchoring groups on the photophysical and photochemical properties were analysed using absorption and cyclic voltammetric measurements. Photovoltaic parameter such as short circuit current density (J_{SC}) and open circuit voltage (V_{OC}) is found to be significantly varied by changing the anchoring unit (Fig. 1).

2 Experimental section

2.1 Equipments and materials

^1H and ^{13}C NMR spectra were recorded on Bruker 400 Ultraschild NMR and CDCl_3 or DMSO-d_6 was used as

solvent. In some cases, Bruker Avance ultra shields 500 MHz were used. FT-IR spectra were recorded in the matrix of KBr with JASCO FT-IR-680 plus spectrometer. Elemental analyses were performed with a Heraeus CHN-O-Rapid analyzer. Mass spectra of the products were obtained with a HP (Agilent technologies) 5937 Mass Selective Detector. Melting points were measured on an electrothermal KSB1 N apparatus. Chemicals were purchased from Aldrich, Fluka and Merck chemical companies.

2.2 Synthesis and characterization of compounds

The starting materials 4-formaltriphenylamine (FTPA), 4,4'-(diformaltriphenylamine (DFTPA), were prepared by adopting literature procedure [14].

2.2.1 Synthesis of 5-(4-diphenylaminophenylmethylene)-2,2-dimethyl-1,3-dioxane-4,6-dione (MM)

To 15 mL of glacial acetic acid were added 150 mg (0.55 mmol) of FTPA and 82.3 mg (0.57 mmol) of Meldrum's acid and the solution was refluxed for 7 h in the presence of 100 mg of ammonium acetate. After cooling to room temperature, the mixture was poured into ice-water. The precipitate was filtered and washed with distilled water. After drying under vacuum, the precipitate was purified by recrystallization from ethanol, obtaining brown crystals of MM (176 mg, 85 %), m.p.180–182 °C. FT-IR (cm^{-1}): 3146, 1716, 1587, 1558, 1489, 1284, 1166, 697. ^1H NMR (500 MHz, CDCl_3 , TMS) δ ppm 8.35 (s, 1H), 7.72 (d, $J = 6.80$ Hz, 2H), 7.38 (q, 4H), 7.20 (t, $J = 10.8$ Hz, 2H), 6.71 (d, $J = 8.0$ Hz, 6H), 1.62 (s, 6H). ^{13}C NMR (125 MHz, CDCl_3) δ ppm 164.3, 146.6, 143.4, 141.3, 140.2, 137.5, 132.1, 128.9, 120.3, 116.8, 113.3, 111.0, 28.3; Mass: m/z 436, 77. Anal.Calcd. For $\text{C}_{25}\text{H}_{21}\text{NO}_4$: C 75.17, H 5.30, N 3.51, O 16.02; found: C 75.14, H 5.28, N 3.49, O 16.00.

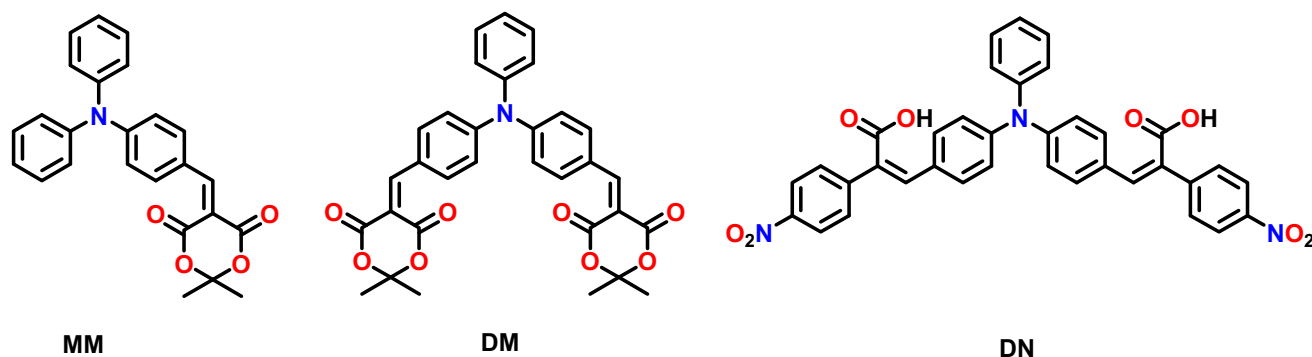


Fig. 1 Molecular structures of MM, DM and DN dyes

2.2.2 Synthesis of 5-{4-[4-(2,2-dimethyle-4,6-dioxo-1,3-dioxan-5-ylidene)methyl](phenyl)anilino]phenylmethylene}-2,2-dimethyl-1,3-dioxane-4,6-dione (DM)

Same as MM but DFTPA (166 mg, 0.55 mmol) instead of FTPA and 164 mg (1.14 mmol) of meldrum's acid were used. The isolated brown powder is DM Yield: 82 %, m.p. 175–177 °C. FT-IR (cm^{-1}): 3156, 1709, 1589, 1506, 1285, 1171, 832, 757, 697. ^1H NMR (DMSO- d_6 , 400 MHz) δ ppm 8.35(d, $J = 8.4$ Hz, 4H), 8.22(s, 2H), 7.43–7.52(m, 2H), 7.01–7.04(q, 1H), 6.88(d, $J = 6.8$ Hz, 6H); ^{13}C NMR (DMSO- d_6 , 100 MHz) δ ppm 164.4, 148.8, 146.2, 143.0, 137.5, 133.0, 130.6, 128.9, 120.3, 116.8, 106.3, 104.1, 27.8.; Mass: m/z 553, 77. Anal. Calcd. For $\text{C}_{32}\text{H}_{27}\text{NO}_8$: C 69.43, H 4.92, N 2.53, O 23.12; found: C 69.39, H 4.89, N 2.52, O 23.10.

2.2.3 (Z)- 3-{4-[4-[(Z)-2-carboxy-2-(4-nitrophenyl)-1-ethenyl](phenyl)anilino]phenyl}-2-(4-nitrophenyl)-2-propenoic acid (DN)

A procedure similar to that for DM but with 4-nitrophenylacetic acid 207 mg (1.14 mmol) instead of meldrum's acid was used. The obtained product was red solid (Yield = 87 %); m.p. 204–206 °C; FT-IR (cm^{-1}): 3432, 1692, 1588, 1505, 1384, 1164, 824.; ^1H NMR (DMSO- d_6 , 400 MHz): δ ppm 11.18 (s, 1H), 8.18 (d, $J = 8.0$ Hz, 4H), 7.68 (s, 2H), 7.46 (d, $J = 8.0$ Hz, 4H), 7.24 (d, $J = 8.0$ Hz, 4H), 6.86 (t, $J = 8.0$ Hz, 3H), 6.26 (d, $J = 8.0$ Hz, 6 H); ^{13}C NMR (DMSO- d_6 , 100 MHz) δ ppm 166.0, 148.0, 146.2, 143.8, 142.1, 130.9, 130.8, 129.7, 121.1, 125.5, 124.7, 124.1.; Mass: m/z 627, 77. Anal. Calcd. For $\text{C}_{36}\text{H}_{25}\text{N}_3\text{O}_8$: C 68.90, H 4.02, N 6.70, O 20.39; found: C 68.85, H 3.98, N 6.68, O 20.36.

2.3 Preparation of TiO_2 electrode

The TiO_2 electrode was prepared according to the reported literature procedure [15]. An amount of 12 g (0.2 mol) of acetic acid was added all at once to 58.6 mg (0.2 mol) of titanium isopropoxide under stirring at room temperature. The modified precursor was stirred for about 15 min and poured into 290 mL water as quickly as possible while vigorously stirring (700 rpm). A white precipitate was instantaneously formed. One hour of stirring was required to achieve a complete hydrolysis reaction. After adding a quantity of 4 mL of concentrated nitric acid, the mixture was heated from room temperature to 80 °C with in 40 min and peptized for 75 min. Water was then added to the cooling liquid mixture to adjust the volume to a final 370 ml. The resultant mixture was kept in a 570 ml titanium autoclave and heated at 250 °C for 12 h. Following

this step, 2.4 ml of 65 % nitric acid was added and the dispersion was treated with a 200 W ultrasonic titanium probes at a frequency of 30 pulses every 2 s. The resultant colloidal solution was concentrated with a rotary-evaporator to contain 13 wt% TiO_2 . Finally, it was triply centrifuged to remove nitric acid and washed with ethanol three times to produce a white precipitate containing 40 wt% TiO_2 in ethanol and only trace amounts of water.

2.4 Fabrication of DSSCs

A thin film of TiO_2 was prepared on the FTO substrate with the compact TiO_2 layer through blade coating. The nanocrystalline TiO_2 working electrode was comprised of a TiO_2 transparent layer (20 nm, synthesized) and a TiO_2 scattering layer (250 nm). The films were then sintered at 500 °C for 1 h. After the film was cooled to room temperature, it was immersed into 3×10^{-4} M solution of the sensitizers in MeCN/*t*-BuOH (1:1, v/v) for 24 h. The sensitized electrode was then rinsed with ethanol and dried. A platinized FTO was prepared by chemical deposition of 0.05 M hexachloroplatinic acid in isopropanol which act as a counter electrode. [16] For the assembly of DSSCs, the dye-covered TiO_2 electrode and Pt-counter electrode were assembled into a sandwich type cell and sealed with a hot-melt gasket of 25 mm thickness made of the ionomer Surlyn 1702 (DuPont). The electrolyte was introduced into the cell via backfilling from a hole in the back of the counter electrode. Finally, the hole was sealed with a cover glass.

2.5 Photo physical and electrochemical measurements

Absorption spectra were measured on a Perkin Elmer (Lambda 25) UV–VIS spectrophotometer. Cyclic voltammetry experiments were performed using a Bio-Logic SP 150 electrochemical analyzer with a scan rate of 100 mVs^{-1} in dimethylformamide (DMF) (3.0×10^{-4} M) containing 0.1 M Bu_4NPF_6 as the supporting electrolyte, platinum wire as counter and working electrodes and Ag/AgCl as reference electrode. Current density–voltage measurements were carried out using simulated 1.5 AM sunlight with an output power of 100 mW cm^{-2} . Electrochemical impedance spectroscopy (EIS) were measured in the frequency range of 10–105 Hz under 1 sun bias illumination under an open-circuit condition using a computer-controlled potentiostat/galvanostat (IVIUM, Compact stat). The incident photon-to-current efficiencies (IPCE) were measured with mono-chromatic incident light of 1×10^{16} photon/ cm^2 under 100 mW cm^{-2} with bias light in DC mode (Jarrel Ash monochromator, using a 100 W halogen lamp) while a calibrated photodiode

(Thorlabs) was used to study the optical properties of layers.

2.6 Theoretical calculation methods

Gaussian 03 package was used for density functional theory calculation. The geometries and energies of MM, DM, and DN were determined using the B3LYP method with the 6-31G (d) basis set.

3 Result and discussion

3.1 Synthesis and characterization of the new dyes

The synthesis of the three new triphenylamine-based organic dyes MM, DM and DN is outlined in Scheme 1.

These dyes contain triphenylamine (TPA) as an electron donor, Meldrum's acid/4-nitrophenylacetic acid group as electron acceptors conjugated through a π -bridge. In the first step the compound TPA was obtained through Ullmann coupling reaction. In the next step, the compound FTPA and DFTPA were synthesized via Vilsmeier reaction. During the formylation reactions, the number of introduced aldehyde groups was controlled by varying the amount of POCl_3 . Finally, the target dyes (MM, DM and DN) were synthesized via Knoevenagel condensation reaction of aldehydes (FTPA, or DFTPA) with Meldrum's acid/4-nitrophenylacetic acid in the presence of CH_3COOH and $\text{CH}_3\text{COONH}_4$. All the intermediates and target dyes were confirmed by standard spectroscopic methods.

3.2 Optical properties

The UV–vis absorption spectra of the dyes MM, DM and DN in THF are shown in Fig. 2 and the results are summarized in Table 1. All the dyes exhibit two absorption peaks: one in below 350 nm, the other in the range of 372–429 nm. The former is due to a localized π – π^* transition and the latter is attributed to the intramolecular charge transfer (ICT) between the TPA donor and the acceptor end group, which provides efficient charge separation at excited state. Di-anchoring dyes (DM and DN) were red-shifted in their absorption spectra, compared to the corresponding mono-anchoring dyes (MM). This is due to the extension of electron delocalization over the whole molecule caused by the introduction of an additional anchoring moiety. The ' ϵ ' for all the compounds is found to be higher than the well-known ruthenium dyes ($<2 \times 10^4 \text{ M}^{-1} \text{ cm}^{-1}$) which can be advantageous of using these sensitizers in photovoltaic applications [11].

The absorption spectra of MM, DM and DN on a TiO_2 film are shown in Fig. 3. The maximum absorption peaks for

MM, DM and DN on the TiO_2 films are about 408, 454 and 408 nm, respectively. The absorption bands of MM, DM and DN dyes on TiO_2 films are red shifted by 36, 25 and 9 nm, respectively, as compared to the bands observed in solution. This red shift can be explained by the formation of J aggregation or the electronic coupling of the dye on the TiO_2 surface [17, 18]. It was reported that a smaller shift in λ_{max} was associated with dyes in solution versus on a thin film, suggesting a smaller tendency to form dye aggregates on the semiconductor surface. This phenomenon results in higher photocurrent densities [19]. It should be noted here that the red shift for dye DN is less than that for dye MM and DM, indicating that the incorporation of the $-\text{COOH}$ acceptor group could effectively suppress the formation of aggregates on the TiO_2 surface. Furthermore, the absorption band of dye DN on the TiO_2 surface became broader compared to that of dye MM because the absorption band of the former might originate from the electronic transition bands of TPA. Therefore, the strong light harvesting ability of dye DN with less aggregation on TiO_2 films is favorable for the performance of DSSCs [20]. The spectra of the dyes were distinctly broadened to longer wavelengths and such a broadening of the absorption spectra is attributable to an interaction between the dyes and TiO_2 surfaces. So, the difference in number and type of anchoring groups in the dyes may result in different arrangement of the dyes on the surface of TiO_2 .

3.3 Electrochemical properties

We have carried out the electrochemical investigations, using cyclic voltammetric technique (see Fig. 4; Table 1) to verify the thermodynamic feasibility of electron injection from the excited state of the dye to conduction band of TiO_2 , and the neutralization of the oxidized dye by accepting electron from I_3^-/I^- redox system.

Suitable highest occupied molecular orbital (HOMO) and lowest unoccupied molecular orbital (LUMO) levels of the sensitizer are crucial for the possibility of electron transfer from the excited dye molecule to the conduction band of TiO_2 . The results are presented in Fig. 4. The derived HOMO and LUMO energies are collected in Table 1 and graphically depicted in Fig. 5. All the observed oxidative waves were reversible.

The highest occupied molecular orbitals (HOMOs) of MM, DM and DN corresponding to their first oxidation potentials (E_{ox}) are 1.76, 1.61 and 1.64 V (vs. NHE), respectively. The band gap energies (E_{0-0}) of the dyes MM, DM and DN were determined to be 3.02, 2.95 and 2.96 V respectively, which comes from the intersections (λ_{int}) of normalized absorption and emission spectra using $E_{0-0} = 1240/\lambda_{\text{int}}$. The lowest unoccupied molecular orbitals (LUMOs) of MM, DM and DN are calculated from $E_{\text{ox}} - E_{0-0}$ to give a value of -1.26 , -1.34 and -1.32 V (vs.

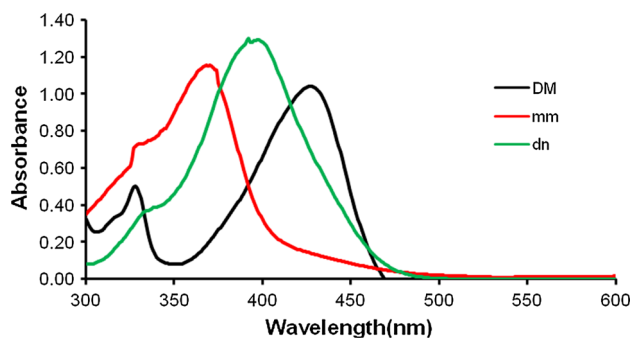
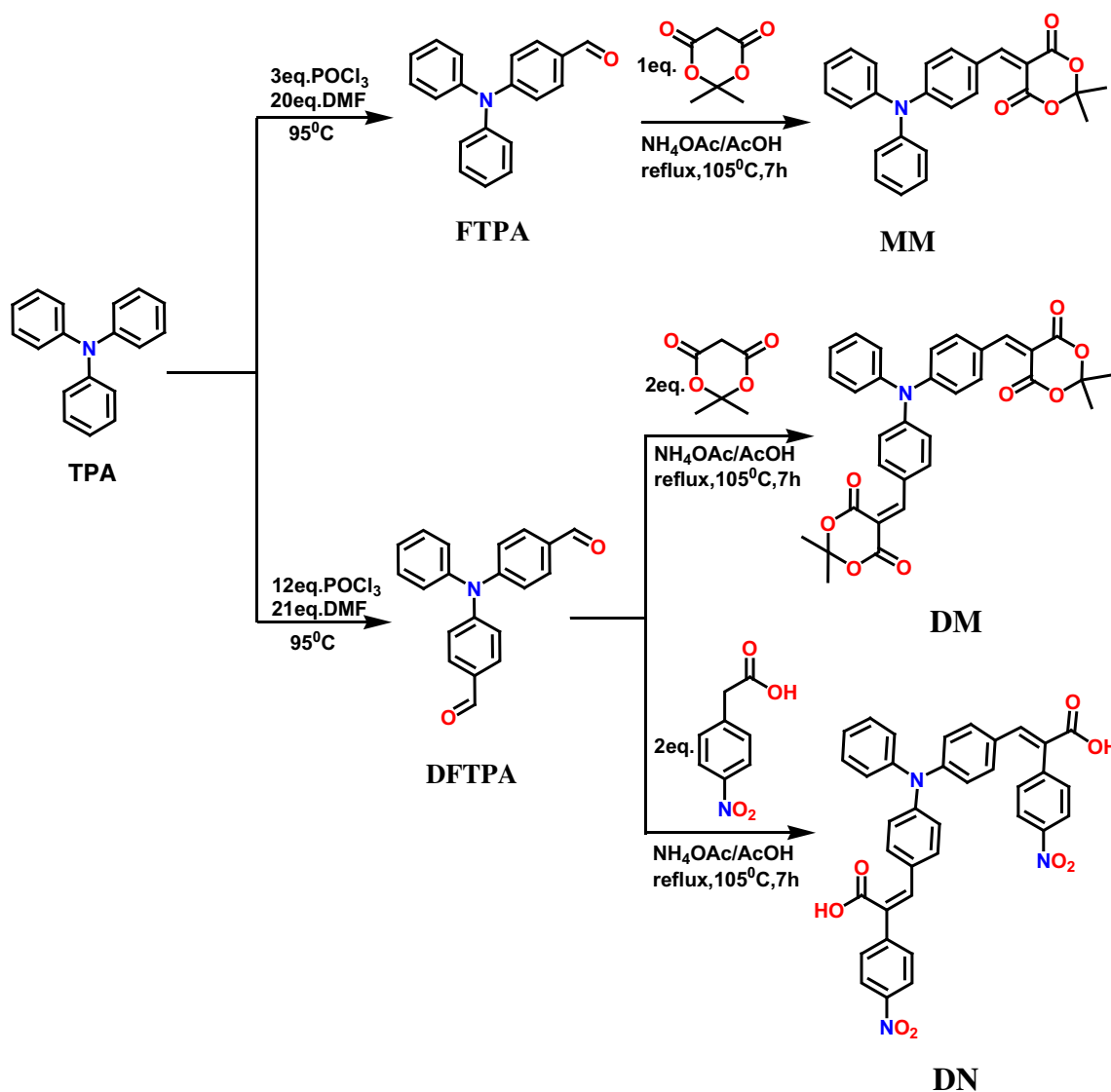


Fig. 2 Absorption spectra of the organic dyes in the THF solution

NHE), respectively. Accordingly, the LUMO levels of MM, DM and DN are more negative than the conduction band (CB) of the TiO_2 electrode (-0.5 V vs. NHE), which is sufficient to provide the required thermodynamic driving

force for electron injection from the dye to the CB of TiO_2 . On the other hand, the HOMO levels of MM, DM and DN are more positive than the redox potential of the iodine/iodide electrolyte (0.4 V vs. NHE), ensuring the regeneration of oxidized dyes.

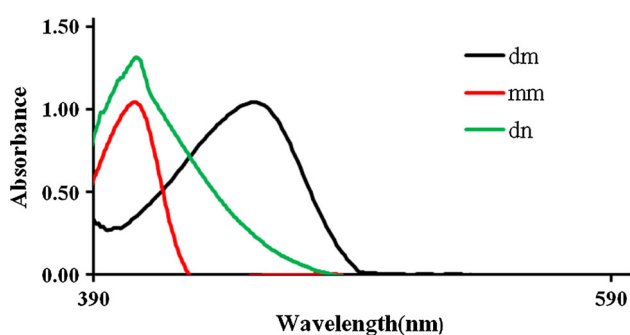
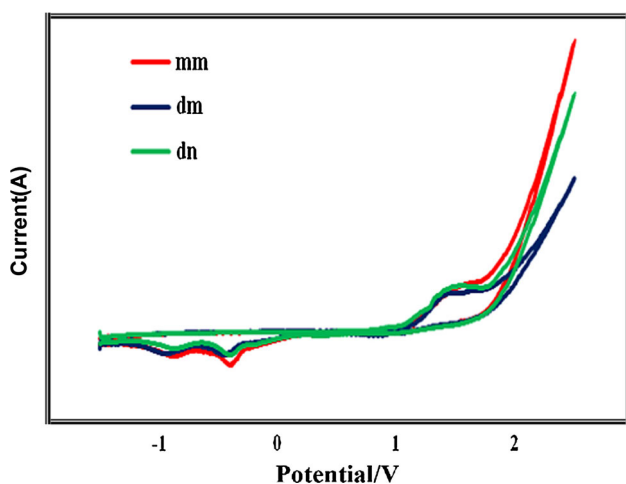
As a consequence, the band gaps of DM and DN were decreased due to the extended π -conjugation unit between the amino donor and meldrum's acid/4-nitrophenylacetic acid groups, compared to MM.

3.4 Molecular orbital calculations

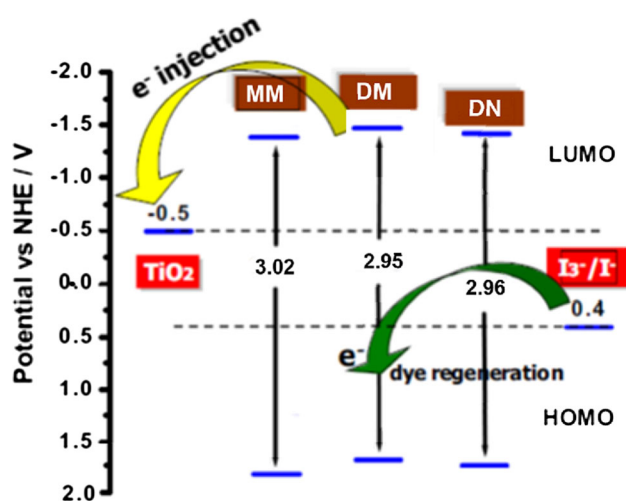
Density functional theory (DFT) calculations were performed on the sensitizers MM, DM and DN to get a deep insight into the structure–photovoltaic cell performance relationships. The calculations were done on a B3LYP/6-31G (d) level for the geometry optimization. The

Table 1 Band gap (calculated by DFT/B3LYP), absorption, and electrochemical parameters for organic dyes

Dye	(HOMO/LUMO) ^a (eV)	(HOMO/LUMO) ^a (eV)	Band gap ^a	($\lambda_{\text{abs}}^{\text{b}}/\text{nm}$)/($\epsilon/10^4 \text{ M}^{-1} \text{ cm}^{-1}$)	$\lambda_{\text{max}}^{\text{c}}/\text{nm}$	HOMO ^d (vs. NHE) (V)	E_{0-0}^{e} (eV)	LUMO ^f (vs. NHE) (V)
MM	-5.09/-3.11	-5.09/-3.11	1.98	372 (3.47)	408	1.76	3.02	-1.26
DM	-5.40/-3.64	-5.40/-3.64	1.76	429 (3.79)	454	1.61	2.95	-1.34
DN	-5.16/-3.68	-5.16/-3.68	1.48	399 (4.31)	408	1.64	2.96	-1.32

^a DFT/B3LYP calculated values^b Absorptions of charge-transfer transition were measured in THF; ϵ absorption coefficient^c Maximum absorption on TiO₂ films^d HOMO of dyes measured by cyclic voltammetry in 0.1 M Bu₄NPF₆ in DMF^e E_{0-0} : 0-0 transition energy measured at the onset of absorption spectra^f LUMO was calculated by HOMO- E_{0-0} **Fig. 3** Absorption spectra of the three dyes absorbed onto TiO₂ film electrodes**Fig. 4** The schematic energy levels of MM, DM and DN based on absorption and electrochemical data

geometries and the electron-density distribution of the highest occupied molecular orbit (HOMO) and the lowest unoccupied molecular orbit (LUMO) of ground-state optimized structures are illustrated in Fig. 6. The HOMOs of MM and DM are delocalized on the entire molecule including donor and acceptor, whereas the LUMOs of these

**Fig. 5** Cyclic voltammograms of the three dyes

molecules are concentrated on the acceptor side of triphenylamine. It should be noted that the LUMO of DM is stretched out to two-anchoring parts of Meldrum's acid which is likely to ensure high electronic coupling between the excited state of dye and TiO₂ conduction band. In contrast, the highest occupied molecular orbital (HOMO) of DN is localized on the triphenylamine unit whereas the lowest unoccupied molecular orbital (LUMO) is localized on the 4-nitrophenylacetic acid group, which is an essential phenomenon for an efficient photoexcited charge transfer to occur [21]. These theoretical results show that the sensitizers can have efficient electron injection from the LUMO to the conduction band of TiO₂ and improving the cell efficiency.

3.5 Photovoltaic device performance

The photovoltaic performance parameters of DSSCs, including short-circuit current density (J_{sc}), open-circuit

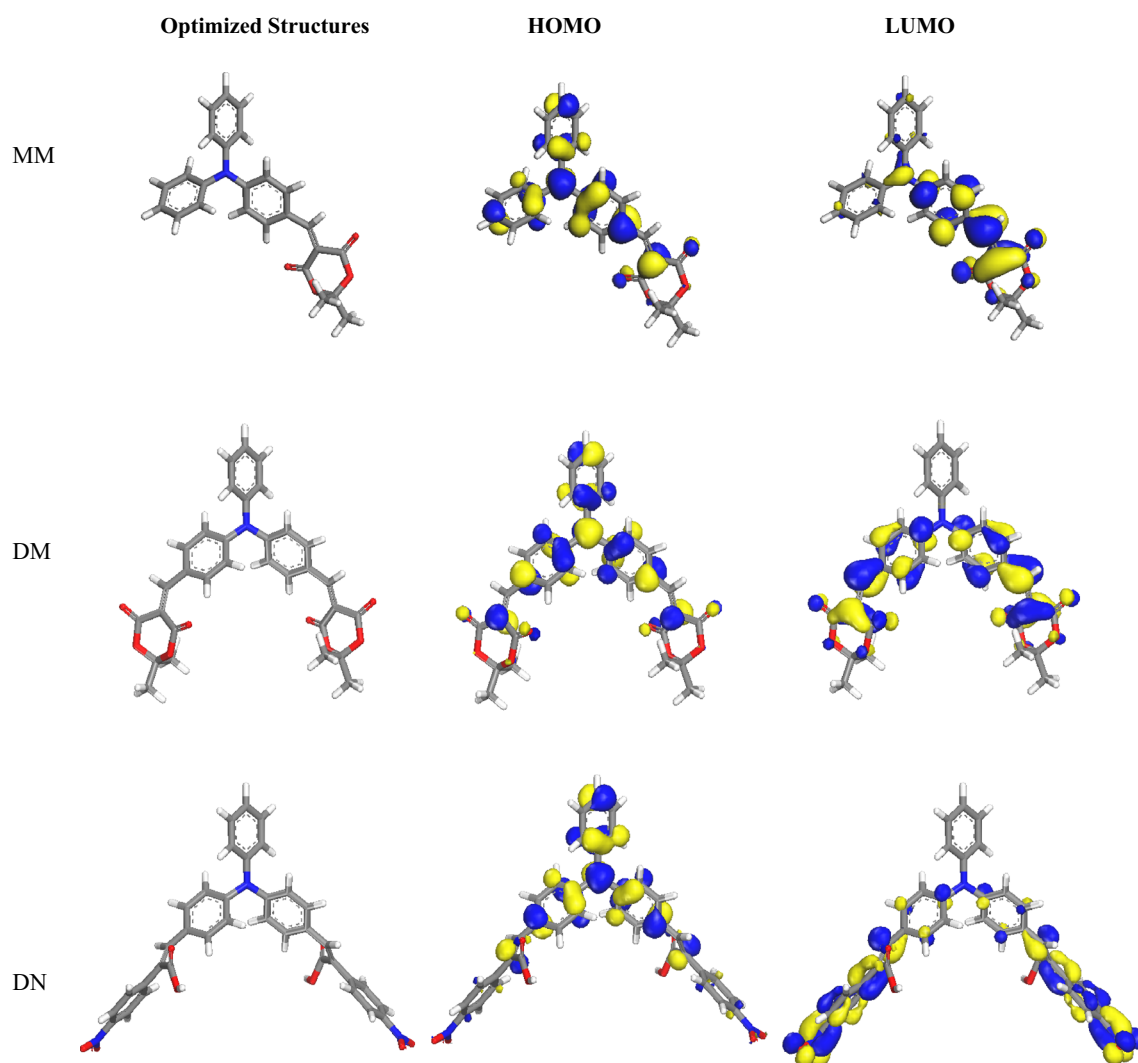


Fig. 6 The frontier molecular orbitals of the HOMO and LUMO levels calculated with B3LYP/6-31G (d) of synthesized dyes

voltage (V_{oc}), fill factor (FF), and power conversion efficiency (PCE) are collected in Table 2, and the J – V curves are shown in Fig. 7. The overall power conversion efficiencies lie in the order of $DM > MM > DN$. The DM-based DSSCs exhibit the highest power conversion efficiency of 2.01 %, while the efficiency of DN-based DSSC is only 0.98 %. The comparison triphenylamine based dyes with single and double anchoring units can be found that the dye with double melderam's acid anchoring units gave 2.01 % efficiency, while the dye with single melderam anchoring unit gave 1.53 %. Double anchoring units in the dye are favorable for electron injection and hence photocurrent generation. According to Fig. 7, it is clear that the photovoltaic performances of the DSSCs can be clearly affected by the anchoring group in the dye molecules. Compared with DN, the conversion efficiencies of solar cells based on MM and DM are significantly increased. The poor photovoltaic performance for DSSC based on DN

Table 2 The performance parameters of the dye-sensitized solar cells

Dye	J_{SC} (mA cm^{-2})	V_{oc} (V)	FF	PCE (%)
MM	3.93	0.55	0.68	1.53
DM	4.58	0.62	0.71	2.01
DN	2.72	0.52	0.69	0.98

with 4-nitrophenylacetic acid as the acceptor is attributed to the following possible characteristics arising from the benzeneacetic acid segment: (1) the relatively short excited electron lifetime (see the electro chemical impedance spectroscopy) and the isolation of LUMO orbital from anchoring group (see the theoretical calculation), resulting in the low photo-excited electron injection efficiency with low J_{SC} ; (2) an overall result of the low injection charge

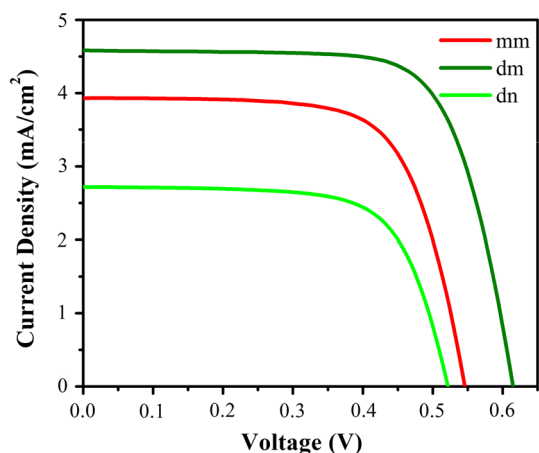


Fig. 7 Photocurrent density vs voltage for DSSCs based on dyes under AM 1.5 G simulated solar light (100 mW cm^{-2})

density in the TiO_2 electrode and fast charge recombination rate between the injected electrons and I_3^- in electrolytes leading to the low V_{OC} . The large J_{sc} could be attributed to the high IPCE values and the broad IPCE spectra.

The incident monochromatic photon-to-current conversion efficiency (IPCE) spectra of the DSSCs are plotted in Fig. 8. The IPCE spectrum of the DSSC follows the absorption spectra of the corresponding dye. It can be seen that the photocurrent response of DM sensitized DSSC is the best due to the IPCE exceeding 90 % in the range of 420–500 nm. The maximum IPCE (98 %) was obtained at 450 nm and this corresponds to almost unity quantum yield when light absorption and reflection by the conducting glass are taken into account. The higher IPCE value of the DSSC based on DM is probably due to a high energy gap between the LUMO level of DM and the conduction band edge of TiO_2 , which leads to an increased electron injection efficiency relative to MM and DN. For MM and DN based DSSCs, lower IPCE values were obtained in the range from 400 to 465 nm and 400 to 467 nm and reached

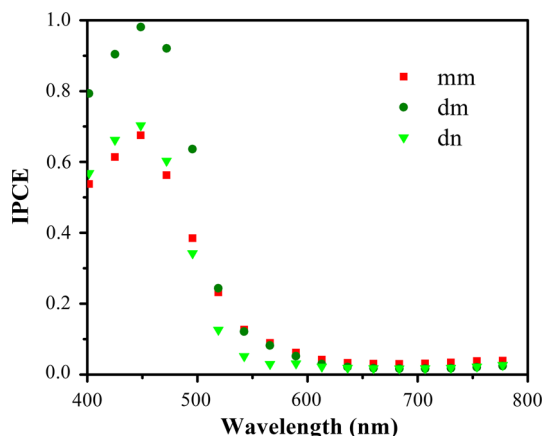


Fig. 8 IPCE spectra of MM, DM and DN

their maximum of 68 % at 450 nm and 70 % at 450 nm, respectively. The decrease of the IPCE above 600 nm toward the long-wavelength region was ascribed to the decrease of light harvesting for three dyes.

Figure 9 shows the electrochemical impedance spectroscopic (EIS) analysis of the cells which is recorded due to a set up whose equivalent circuit is represented in Fig. 9b. The results of EIS data fits listed in Table 3. R_{ct} , τ and $C\mu$ correspond to the charge transfer process occurring at the $\text{TiO}_2/\text{dye}/\text{electrolyte}$ interface, electron life time and chemical capacitance, respectively. CPE ct-T and CPE ct-P are parameters of constant phase elements charge transfer (CPE ct).

Electrochemical impedance spectroscopy (EIS) successfully models the charge transfer and chemical capacitance at the interface of $\text{TiO}_2/\text{dye}/\text{electrolyte}$ and $\text{pt}/\text{electrolyte}$ in DSSC under operational conditions [22–24]. The Nyquist plots for the DSSCs based on MM, DM and DN are displayed in Fig. 9a. The first semicircle (R_{ce}) is attributed to charge transfer at the counter electrode/electrolyte interface, while the second semicircle (R_{rec}) is accorded to charge transfer at the $\text{TiO}_2/\text{dye}/\text{electrolyte}$ interface [23]. The similar R_{ce} values (for MM, DM and DN) were probably due to the same counter electrode and electrolyte. A large R_{rec} means a small dark current and a low charge recombination rate [25]. The R_{rec} values for MM, DM and DN were estimated to be 20.18, 19.39 and 30.57, respectively, as shown in Table 3. Obviously, the R_{rec} value of DN was much larger than the other two dyes, which could restrain the charge recombination between injected electron and electron acceptor (I_3^-) in the electrolyte, thereby contributing to the V_{oc} [26].

By fitting the EIS curves, another important parameters for DSSCs, electron lifetime (τ), could be extracted from the

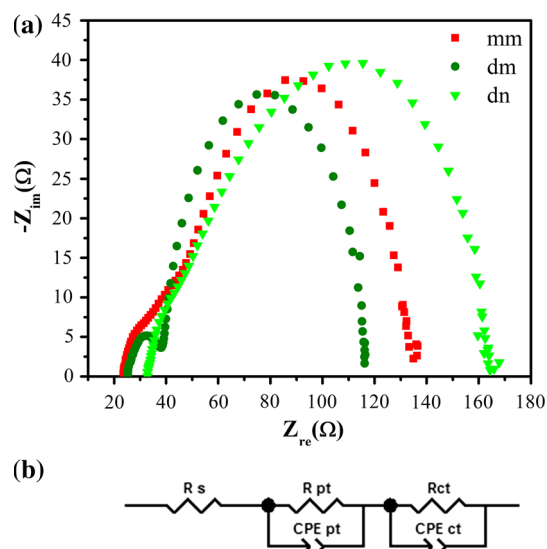


Fig. 9 Electrochemical impedance spectra (a-Nyquist plot; b-equivalent circuit for a) of DSSCs for three dyes

Table 3 EIS parameters obtained from modelling the EIS result

Dye	R_{ct} (Ω cm ²)	CPE ct-T (10^{-4})	CPE ct-P	τ (ms)	C_{μ} (10^2 μ F cm ⁻²)
MM	20.18	4.01	0.91	23.22	11.50
DM	19.39	5.11	0.94	32.76	16.89
DN	30.57	2.18	0.72	6.48	2.12

chemical capacitances (C_{μ}) and R_{CT} using $\tau = C_{\mu} \times R_{ct}$. So the trend of electron lifetimes was in the order of $DM > MM > DN$, which was well in accordance with the changing tendencies of V_{oc} values obtained in J - V curves. Evidently, the longer electron lifetime of DM compared to the other two dyes could suppress the generation of dark current and reduce electron recombination more effectively, resulting in a higher V_{oc} in DM-based device [27].

The higher electron lifetime indicates suppression of back reaction of the electrons with the I_3^- in the electrolyte and this was reflected in the improvements of the photocurrent, yielding substantially enhanced device efficiency for the DSSCs based on DM as compared to MM and DN.

4 Conclusion

Triphenylamine based sensitizers (MM, DM and DN) with two new electron withdrawing anchoring group were synthesized and characterized by FT-IR, ¹H, ¹³C NMR, Mass spectral and CHN analysis. Also all photophysical, electrochemical and photovoltaic properties have been studied.

As a result, DM outperforms the other two sensitizers, exhibiting power conversion efficiency of 2.01 %, with J_{sc} of 4.58 mA cm⁻² and V_{oc} of 0.62 V under simulated AM 1.5 irradiation (100 mW cm⁻²). Whereas, dye DN with 4-nitrophenylacetic acid as the anchoring group delivers the lowest power conversion efficiency, due to its poor absorption on TiO₂ film, its shorter electron lifetime and the fast charge recombination from the EIS results.

These sensitizers could be mixed with other sensitizers with optimized red response in a tandem arrangement to achieve excellent photoconversion efficiencies in the spectral regions of interest. All the results indicate that these organic compounds are promising candidates in the development and further optimization of metal-free organic sensitizers for application in DSSCs.

Acknowledgments We are grateful to the Yasouj University, industrial Sharif University for financial supports.

References

1. B. O'Regan, M. Gratzel, A low-cost, high-efficiency solar cell based on dye-sensitized colloidal TiO₂ films. *Nature* **353**, 737–740 (1991)

2. M.K. Nazeeruddin, A. Kay, A.I. Rodicio, R. Humphry-Baker, E. Muller, P. Liska, N. Vlachopoulos, M. Gratzel, Conversion of light to electricity by cis-X2bis(2,2'-bipyridyl-4,4'-dicarboxylate)ruthenium(II) charge-transfer sensitizers (X = Cl⁻, Br⁻, I⁻, CN⁻, and SCN⁻) on nanocrystalline titanium dioxide electrodes. *J. Am. Chem. Soc.* **115**, 6382–6390 (1993)
3. M.K. Nazeeruddin, S.M. Zakeeruddin, R. Humphry-Baker, M. Jirousek, P. Liska, N. Vlachopoulos, V. Shklover, C.H. Fisher, M. Gratzel, Acid–base equilibria of (2,2'-bipyridyl-4,4'-dicarboxylic acid)ruthenium(II) complexes and the effect of protonation on charge-transfer sensitization of nanocrystalline titania. *Inorg. Chem.* **38**, 6298–6305 (1999)
4. M.K. Nazeeruddin, P. Pechy, T. Renouard, S.M. Zakeeruddin, R. Humphry-Baker, P. Comte, P. Liska, L. Cevey, E. Costa, V. Shklover, L. Spiccia, G.B. Deacon, C.A. Bignozzi, M. Gratzel, Engineering of efficient panchromatic sensitizers for nanocrystalline TiO₂-based solar cells. *J. Am. Chem. Soc.* **123**, 1613–1624 (2001)
5. W. Zeng, Y. Cao, Y. Bai, Y. Wang, Y. Shi, M. Zhang, F. Wang, C. Pan, P. Wang, Efficient dye-sensitized solar cells with an organic photosensitizer featuring orderly conjugated ethylenedioxythiophene and dithienosilole blocks. *Chem. Mater.* **22**, 1915–1925 (2010)
6. K. Sayama, S. Tsukagoshi, K. Hara, Y. Ohga, A. Shinpou, Y. Abe, S. Suga, H. Arakawa, Photoelectrochemical properties of j aggregates of benzothiazole merocyanine dyes on a nanostructured TiO₂ film. *Phys. Chem. B* **106**, 1363–1371 (2002)
7. Z.-S. Wang, F.-Y. Li, C.-H. Huang, Photocurrent enhancement of hemicyanine dyes containing RSO₃⁻ group through treating TiO₂ films with hydrochloric acid. *Phys. Chem. B* **105**, 9210–9217 (2001)
8. K. Kalyanasundaram, M. Grätzel, Applications of functionalized transition metal complexes in photonic and optoelectronic devices. *Coord. Chem. Rev.* **177**, 347–414 (1998)
9. D. Liu, R.W. Fessenden, G.L. Hug, P.V. Kamat, Dye capped semiconductor nanoclusters. Role of back electron transfer in the photosensitization of SnO₂ nanocrystallites with cresyl violet aggregates. *Phys. Chem. B* **101**, 2583–2590 (1997)
10. N. Koumura, Z.S. Wang, S. Mori, M. Miyashita, E. Suzuki, K. Hara, Alkyl-functionalized organic dyes for efficient molecular photovoltaics. *J. Am. Chem. Soc.* **128**, 14256–14257 (2006)
11. K.R.J. Thomas, A. Baheti, P. Singh, C.P. Lee, K.C. Ho, 2,7-Diaminofluorene-based organic dyes for dye-sensitized solar cells: effect of auxiliary donor on optical and electrochemical properties. *J. Org. Chem.* **76**, 4910–4920 (2011)
12. J.K. Lee, M. Yang, Progress in light harvesting and charge injection of dye-sensitized solar cells. *J. Mater. Sci. Eng. B.* **176**, 1142–1160 (2011)
13. S.Y. Qu, J.L. Hua, H. Tian, New D- π -A dyes for efficient dye-sensitized solar cells. *Sci. China Chem.* **55**, 677–697 (2012)
14. M. Behl, E. Hattermer, M. Brehmer, R. Zentel, Tailored semiconducting polymers: living radical polymerization and NLO-functionalization of triphenylamines. *Macromol. Chem. Phys.* **203**, 503–510 (2002)
15. S. Ito, T. Murakami, P. Comte, P. Liska, C. Grätzel, M. Nazeeruddin, M. Grätzel, Fabrication of thin film dye sensitized solar cells with solar to electric power conversion efficiency over 10 %. *Thin Solid Films* **516**, 4613–4619 (2008)

16. Q. Wang, S. Ito, M. Gratzel, F. Fabregat-Santiago, I. Mora-Sero, J. Bisquert et al., Characteristics of high efficiency dye-sensitized solar cells. *J. Phys. Chem. B* **110**, 25210–25221 (2006)
17. X. Ren, Q. Feng, G. Zhou, C.-H. Huang, Z.S. Wang, Effect of cations in coadsorbate on charge recombination and conduction band edge movement in dye-sensitized solar cells. *J. Phys. Chem. C* **114**, 7190–7195 (2010)
18. J. Tang, J.L. Hua, W.J. Wu, J. Li, Z.G. Jin, Y.T. Long, H. Tian, New starburst sensitizer with carbazole antennas for efficient and stable dye-sensitized solar cells. *Energy Environ. Sci.* **3**, 1736–1745 (2010)
19. S. Roquet, A. Cravino, P. Leriche, O. Alévêque, P. Frere, J. Roncali, Triphenylamine-thienylenevinylene hybrid systems with internal charge transfer as donor materials for heterojunction solar cells. *J. Am. Chem. Soc.* **128**, 3459–3466 (2006)
20. C. Teng, X. Yang, C. Yang, H. Tian, S. Li, X. Wang, A. Hagfeldt, L. Sun, Influence of triple bonds as π -spacer units in metal-free organic dyes for dye-sensitized solar cells. *J. Phys. Chem. C* **114**, 11305–11313 (2010)
21. W.M. Campbell, A.K. Burrell, D.L. Officer, K.W. Jolley, Porphyrins as light harvesters in the dye-sensitized TiO_2 solar cell. *Coord. Chem. Rev.* **248**, 1363–1379 (2004)
22. R. Kern, R. Sastrawan, J. Ferber, R. Stangl, J. Luther, Modeling and interpretation of electrical impedance spectra of dye solar cells operated under open-circuit conditions. *Electrochim. Acta* **47**, 4213–4225 (2002)
23. Q. Wang, J. Moser, M. Gratzel, Electrochemical impedance spectroscopic analysis of dye-sensitized solar cells. *J. Phys. Chem. B* **109**, 14945–14953 (2005)
24. N. Koide, A. Islam, Y. Chiba, L. Han, Improvement of efficiency of dye-sensitized solar cells based on analysis of equivalent circuit. *J. Photochem. Photobiol. A* **182**, 296–305 (2006)
25. M. Cheng, X. Yang, J. Li, C. Chen, J. Zhao, Y. Wang, L. Sun, Dye-sensitized solar cells based on a donor–acceptor system with a pyridine cation as an electron-withdrawing anchoring group. *Chem. Eur J.* **18**, 16196–16202 (2012)
26. D. Wang, W. Ying, X. Zhang, Y. Hu, W. Wu, J. Hua, Near-infrared absorbing isoindigo sensitizers: synthesis and performance for dye-sensitized solar cells. *Dyes Pigments* **112**, 327–334 (2015)
27. Z. Huang, H. Feng, X. Zang, Z. Iqbal, H. Zeng, D. Kuang, L. Wang, H. Meier, D. Cao, Dithienopyrrolobenzothiadiazole-based organic dyes for efficient dye-sensitized solar cells. *J. Mater. Chem. A* **2**, 15365–15376 (2014)